mmFruit: A Contactless and Non-Destructive Approach for Fine-Grained Fruit Moisture Sensing Using Millimeter-Wave Technology

Fahim Niaz, Jian Zhang, Muhammad Khalid, Muhammad Younas, and Ashfaq Niaz,

***Abstract*—Wireless sensing offers a promising approach for non-destructive and contactless identification of the moisture content in fruits. Traditional methods assess fruit quality based on external features such as color, shape, size, and texture. However, fruits often appear perfect externally while being rotten inside. Thus, accurately measuring internal conditions is crucial. This paper introduces mmFruit, a non-destructive and ubiquitous system that employs mmWave signals for precise and robust moisture level sensing in thin and thick pericarp fruits. We propose a novel dual incidence moisture estimation model for regular moisture monitoring to achieve high granularity and eliminate fruit type and size dependency. Additionally, we leverage unique reflection responses across different mmWave frequencies to provide discriminative information about fruit moisture levels. Our comprehensive theoretical model demonstrates how fruits' refractive index, attenuation factor, and elasticity can be estimated by eliminating fruit type dependency. We developed an electric field distribution model utilizing two receiving antennas to address the challenge of varying fruit sizes through a differential approach, aiming to improve overall robustness. mmFruit integrates a customized Spatial-invariant network (SpI-Net) to eliminate interference from different frequencies and locations, ensuring stable moisture monitoring regardless of target displacement. Extensive experiments were conducted over a month in varied environments on seven types of fruits with thin and thick pericarps (apple, pear, peach, mango, orange, dragon fruit, and watermelon). The results demonstrate that mmFruit achieves a commendable RMSE of 0.276 in moisture estimation. It accurately distinguishes fruits with minor moisture level differences (0% to 7%) with 93.6% accuracy and higher moisture differences (45% to 65%) with over 95.1% accuracy, even in scenarios involving diverse displacements and rotations.**

***Index Terms*—Millimeter Wave, Wireless Sensing, Contact-less Sensing, Moisture Sensing**

I. Introduction

Fruits are rich in carbohydrates, amino acids, proteins, organic acids, vitamins, and minerals, making them a valuable part of the human diet. It is recommended to consume them fresh. However, many fruits are perishable due to their high metabolism, respiration rate, and limited shelf life (1). Improving post-harvest management of fresh fruit is crucial for enhancing food supply (2). Unfortunately, post-harvest processing often results in the loss of several beneficial nutrients. External and internal factors such as temperature and humidity during storage, significantly impact quality and shelf life, influencing attributes like firmness, weight loss, titratable acidity, and soluble solid concentration (3), (4). Pathogenic microbes also significantly influence fruit spoilage and shelf life reduction. Despite advancements in bactericidal treatments, many infectious disorders remain challenging to manage due to bacterial resistance, low cell activity, antimicrobial toxicity to healthy tissues, and difficulty crossing cell membranes. Therefore, developing more effective materials with enhanced photocatalytic and antibacterial properties is essential (5).

Evaluating the quality of fruit involves both external and internal factors. External characteristics like color, shape, size, and the absence of surface bruises can be visually inspected and are commonly used to assess fruit quality in daily life (6). Vision-based fruit sorting systems also utilize these external features for classifying fruit freshness (7). However, relying solely on external factors can be misleading, as fruit may look normal on the outside but be rotten inside. A critical internal factor is the measurement of moisture level in fruit, which helps reduce this bias. Commodity-of-the-shelf (COTS) analyzers often employ destructive testing methods. Tools such as penetrometers (8), (9) and vacuum ovens (10) measure water content by inserting probes and applying heat to dry the fruit. In contrast, nondestructive techniques analyze moisture levels by examining the absorption, reflection, and scattering of near-infrared (NIR) signals emitted to the fruit tissues. Professional spectrometers (11) provide relatively accurate measurements (±1.7% for moisture) but are costly (approximately $100,000) and require controlled laboratory settings (12). Although portable spectrometers are less expensive (around $9,000) (13), they do not achieve satisfactory accuracy across different types of fruits.

RF-based fruit sensing has been explored to circumvent the need for destructive and expensive methods for measuring internal fruit properties. RF waves experience varying velocity loss and propagation attenuation degrees when passing through fruits with different moisture levels. A machine learning-based system for classifying fruit moisture levels (14) is developed using terahertz (THz) waves in the 0.75-1.1 THz

Manuscript received. The paper is submitted to the IEEE Transactions on Mobile Computing. This paper presents mmFruit: A Contactless and Non-Destructive Approach for Fine-Grained Fruit Moisture Sensing Using Millimeter-Wave Technology.

Fahim Niaz, Wuhan University, Wuhan China (e-mail: notify.fahim@outlook.com).
Jian Zhang is the corresponding author, Wuhan University, Wuhan China (e-mail: jzhang@whu.edu.cn).
Muhammad Khalid, University of Hull, Hull UK (e-mail: M.Khalid@hull.ac.uk).
Muhammad Younas, Wuhan University, Wuhan China (e-mail: younas@whu.edu.cn).
Ashfaq Niaz, Taiyuan University of Technology, Taiyuan China (e-mail: ashfaq123niaz@gmail.com).

range. However, this system requires a specialized platform like Swissto12 MCK, limiting its practicality for everyday use. A wi-fi-based system for creating fruit ripeness profiles using a 600MHz bandwidth at 5GHz was developed (15). Still, it failed to provide detailed measurements of biological features such as moisture values. The state-of-the-art model, Wi-Fruit (16), utilizes a COTS Wi-Fi device with dual antennas to estimate various fruits' moisture levels and solid-state content. However, this method relies heavily on visual information, necessitating images for fruit type, and size to ensure accuracy.

In this paper, we introduce mmFruit, a novel system designed to non-destructively measure fruit moisture levels using a dual incidence moisture estimation model. It utilizes a mmWave radar device (77-81 GHz) to transmit Frequency-Modulated Continuous Wave (FMCW) chirps toward fruits at normal and oblique angles. By analyzing the reflected signals, mmFruit accurately measures and monitors fruit moisture levels using the refractive index to gauge how much the radar signal bends within the fruit and the fruit's elasticity to determine how the fruit's firmness correlates with moisture content. It can detect subtle moisture differences between 0% and 7%, as well as significant variations between 45% and 65%. To eliminate fruit type dependency, we developed a feature based on attenuation factors independent of fruit type. We constructed an electric field around the radar's receiving antennas to detect fruit size. mmFruit reliably operates in diverse real-world conditions, including random movements and rotations, making it invaluable for retailers and consumers seeking precise moisture level information.

To achieve accurate and resilient moisture level sensing, mmFruit introduces two unique design innovations:

1) Our dual incidence moisture estimation model enhances mmFruit's capability to achieve fine-grained measurements by utilizing both normal and oblique reflection incidences. This approach leverages distinct reflection characteristics across various frequencies, overcoming the limitations of existing methods that rely on visual information about fruit type, size, and normal incidence reflection features. mmFruit capitalizes on the varying moisture permittivity across multiple mmWave frequencies to derive reflection coefficients, refractive indices, fruit attenuation factors, and fruit elasticity. This allows for regular moisture monitoring and provides detailed insights into the fruit's type, size, and moisture level. By capturing diverse frequency characteristics from FMCW mmWave signals, the proposed dual incidence moisture estimation model enables accurate detection and utilization of detailed moisture information reflected across different mmWave frequencies.
2) Mitigating interference from range bin changes and rotation using Spatial-invariant networks (SpI-Net). To ensure reliable moisture level sensing and address interference caused by different displacements under normal and oblique incidences, mmFruit integrates a customized neural network called SpI-Net. SpI-Net extracts location-independent features uniformly by employing shared convolutional kernels with residual connections and consistent learnable parameters. This methodology allows SpI-Net to capture and down-sample reflection responses across various range bins, effectively extracting invariant features and enhancing the accuracy of moisture identification.

In summary, The major contributions of mmFruit are:

- We develop a dual incidence moisture estimation model that establishes a functional relationship between fruit moisture levels and the refractive index of received signals at both normal and oblique incidences. By analyzing the electric field differences when the spatial position of the fruit changes, we extract reflection coefficients and refractive indexes. This approach enables the accurate identification of moisture levels.
- We introduce mmFruit, a system for regularly monitoring fruit moisture content using fruit elasticity, defined as the ratio of stress to strain. mmFruit can detect minor moisture changes (0%-7%) and major moisture variations (45%-65%) with an RMSE of 0.276, even among similar moisture-content fruits like pears and apples.
- To eliminate the effect of fruit type, we utilize each fruit type's complex permittivity and fruit attenuation factors, which vary with frequency. We design a relative frequency response factor, based on the attenuation factors at multiple frequencies, to counteract the influence of fruit type. By leveraging relative complex permittivity and the frequency response factor as features, mmFruit can accurately identify fruit types without relying on visual information.
- We developed a customized Spatial-Invariant Network (SpI-Net) to consistently monitor moisture levels in fruits, effectively mitigating the effects of location changes and ensuring robust moisture identification. The mmFruit prototype, built using mmWave radar, is designed to interface seamlessly with any smart device. We collected over 58,000 samples for extensive experiments and case studies, confirming the prototype's accuracy and robustness across various scenarios.

II. Related Work

Non-destructive evaluation (NDE) of agricultural products has become increasingly important over the past few decades. About 50 years ago, initial studies used microwaves in agriculture showing that the complex permittivity of fruits and vegetables varied with their maturity and type through destructive methods (17), (18). Today, the focus is on using microwaves for non-destructive monitoring of fruit growth and maturity. Recent research highlights the use of microwaves to measure the mass of products like grapes (19) and cranberries (20), (21) and to determine the best harvest time based on fruit maturity. Additionally, electronic-based techniques like electronic noses (22) and tongues (23) are being developed for flavor assessment.

Recent advancements in RF-based technologies (24), (25), have become increasingly important for non-destructive fruit quality assessment, encompassing both external and internal evaluations. External factors include fruit type, size, shape, weight, firmness, smell, surface color, and features like mildew spots. The Doppler laser vibrometer (LDV) (26) accurately measures changes in fruit surface texture using reflected laser beams. Vision-based technology (27) is also widely used for external evaluations, employing image processing and deep learning. However, their performance can be affected by environmental lighting conditions.

Assessing fruit quality based only on external factors can be misleading. Internal factors are also important, such as moisture, soluble solids content (SSC), water activity, fat content, and fiber. Spectroscopy (28) is a traditional method for analyzing the internal patterns of fruit using electromagnetic radiation. It emits NIR signals to the surface of the fruit and examines its internal features based on varying degrees of absorption, reflection, and scattering. Although spectrometers offer non-destructive internal measurements, they are often expensive and require controlled environments. Another method for non-destructive internal assessment is ultrasound-based sensing. Researchers (29) have used mechanical waves with programmable bipolar remote ultrasonic pulse generators to measure fruit color and hardness, achieving about 82% accuracy.

In contrast, RF-based methods offer non-destructive sensing of fruit with easier deployment, lower cost, and relatively high accuracy. Recent advancements in mmWave signal-based ubiquitous sensing include Securing Pattern Lock (30), Speech Recognition System (31), vocal sensing system (32), vital signs monitoring (33), and Alcohol Sensing (34). The short wavelength of mmWave signals allows for high-resolution perception. Recent studies have used lightweight and compact mmWave radar hardware for material identification by common users. Additionally, Wi-Fi-based material sensing has been explored for baggage detection, liquid level sensing (35), and currency detection (36), (37). Yet, these methods are not directly suitable for the nuanced requirements of fruit quality assessment.

III. Motivation

This section first discusses various everyday scenarios for measuring fruit moisture levels. We then review existing commercial off-the-shelf (COTS) devices and research efforts in this area. We analyze the significant challenges associated with current methods and introduce mmWave technology for moisture measurement, which motivates the design of mmFruit.

A. Potential Scenarios for Moisture Measurements

The moisture level is crucial for assessing fruit quality and can enhance storage practices in various ways:

- **Home storage optimization**: Regular moisture monitoring with a handheld or home-based mmWave device can help consumers store fruit under optimal conditions, preserving freshness and reducing spoilage. By knowing moisture content, users can better decide how to use each fruit; for example, high-moisture fruits are ideal for juicing, while low-moisture ones work well for baking. This approach extends fruit shelf life and minimizes food waste.

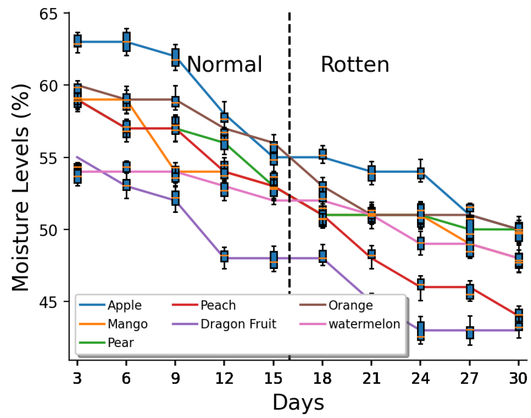

Fig. 1: Analysis of fruit moisture levels over time: normal vs. rotten.

- **Providing fruit shelf life**: Tracking moisture changes over time helps prevent spoilage. As shown in Fig. 1, fruits follow a consistent moisture trend as they near spoilage, typically within 7-15 days. By calculating this rate, consumers can estimate freshness and know when to consume fruit before it over-ripens. This practical solution helps households manage storage efficiently, reducing waste and enhancing quality.

B. Existing Methods Challenges, and Role of mmWave in Fruit Moisture Measurement

Existing COTS devices for measuring fruit moisture levels are summarized in Tab. I. Portable penetrometers (9) estimate moisture by measuring the voltage difference between two probes inserted into the fruit tissue. This method is direct but limited because it only measures one internal feature and is destructive to the fruit. Also, laboratory vacuum ovens (10) offer more accurate water content measurements by drying fruit samples under controlled conditions. While precise, this method also has limitations as it can only assess a single feature and requires the fruit to be destroyed. On the other hand, spectrometers (13) provide a non-destructive way to assess internal fruit quality, measuring both moisture and soluble solids content (SSC). Despite their effectiveness, spectrometers are relatively expensive, costing between $9,000 and $100,000, as shown in Table 1. This high cost makes them impractical for everyday use.

RF waves passing through fruit experience different levels of attenuation based on the fruit's moisture content, allowing moisture measurement using RF signals. (15) developed fruit ripeness profiles using RF spectra of 0.75-1.1 THz to investigate fruit moisture. Wi-Fruit (16) introduced a double-quotient model-based CSI Pre-processing to reduce interference from sensor-target distance changes, enabling non-destructive and affordable moisture and SSC measurements with Wi-Fi. However, these methods did not provide a detailed internal feature analysis of the fruit and relied on visual images.

We introduce mmFruit, a novel method for precise fruit moisture estimation using mmWave radar. To the best of our

TABLE I: Comparison of COTS devices typically used for measuring fruit moisture levels with the proposed mmFruit model.

System	Device	Normal/Oblique	Type Independent	Size Independent	Distance Independent	Non-Destructive
Penetrometer (9)	Jacks JK-100R	Normal	✗	✗	✗	✗
Vacuum Oven (10)	Yamato ADP-31	Normal	✗	✗	✗	✓
Spectrometer (13)	MoisTech-IR-3000R	Normal	✗	✗	✗	✓
TeraHertz (14)	Swissto 12	Normal	✗	✗	✗	✗
Wi-Fruit (16)	Wi-Fi 20MHz	Normal	✗	✗	✗	✓
mmFruit	**TI-IWR1443**	**Normal/Oblique**	✓	✓	✓	✓

knowledge, mmFruit is the first system to deliver accurate fruit moisture measurements at normal and oblique incidence, independent of fruit type and size. It provides non-destructive, contactless sensing, allowing moisture measurement without damaging the fruit, unlike invasive techniques. The high spatial resolution of mmWave signals captures fine-grained moisture variations within fruit layers, enhancing accuracy. Additionally, it is robust in varying environmental conditions, performing consistently across different storage environments and being less affected by changes in light, temperature, and humidity (38). Unlike optical methods, it can penetrate shallowly beneath the surface, reducing sensitivity to variations in surface texture and skin type, making it suitable for a wide range of fruit types. These advantages make mmFruit an ideal choice for reliable, non-invasive moisture measurement.

The following sections detail the theoretical model for moisture sensing, highlighting the reflection feature extraction at both normal and oblique incidence.

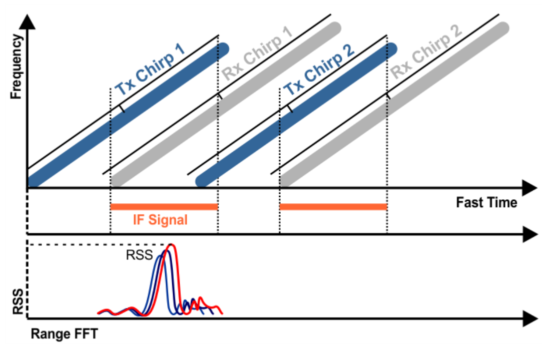

Fig. 2: mmWave Frequency-Modulated Continuous Wave (FMCW) chirps.

IV. Preliminaries

In this section, we introduce the fundamental principles of mmWave radar and the key physical properties used for moisture estimation.

A. mmWave Radar Fundamentals

mmWave radar systems typically utilize the FMCW technique to detect objects in their vicinity. As illustrated in Fig. 2, the radar emits continuous mmWave signals over short intervals called chirps, during which the transmitted signal frequency increases linearly. The transmitting signal frequency $R_T(\alpha)$ over time α can be expressed as:

$$R_T(\alpha) = f_c + G\alpha \tag{1}$$

where f_c is the starting frequency and G represents the chirp slope. Signals reflected from an object located at a distance d will have a frequency given by:

$$R_R(\alpha) = R_T\left(\alpha - \frac{2d}{C}\right) \tag{2}$$

where C is the speed of light. Mixing the transmitted and received signals produces an Intermediate Frequency (IF) signal R_{IF}, which remains constant:

$$R_{IF} = \frac{2dG}{C} \tag{3}$$

In a radar system with a constant chirp slope G, the IF signal R_{IF} frequency is directly proportional to the distance d of the radar target. By applying the Fast Fourier Transform (FFT) to the IF signals with different frequencies, the FMCW radar can accurately distinguish and measure targets at varying distances.

B. Range Estimation

The sensing capability of a mmWave radar system depends primarily on its transmitting and receiving antennas. The transmitting antennas emit signals into the environment, while the receiving antennas capture the signals reflected from nearby objects. By analyzing the frequency difference between the transmitted and received signals (illustrated in Fig. 2), the distance to the target can be determined by

$$R = \frac{Cf}{2G} \tag{4}$$

where C is the speed of light. The range resolution indicates how well the radar can distinguish between two nearby targets. The size must be larger than the radar's range resolution to differentiate the signals reflected from background objects and the fruit. In case the bandwidth is 4 GHz, the range resolution is around 4 cm, given a bandwidth B, the range resolution R_{rs} can be expressed as

$$R_{rs} = \frac{C}{2G} \tag{5}$$

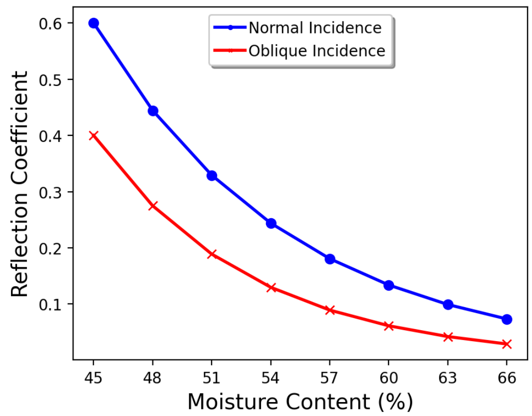

Fig. 3: Theoretical measurements of the reflection coefficient.

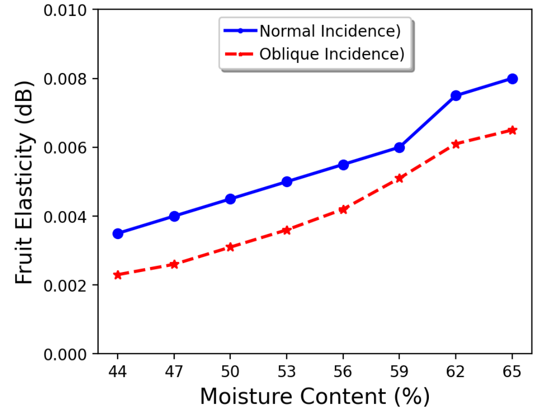

Fig. 5: Fruit elasticity at varying moisture levels.

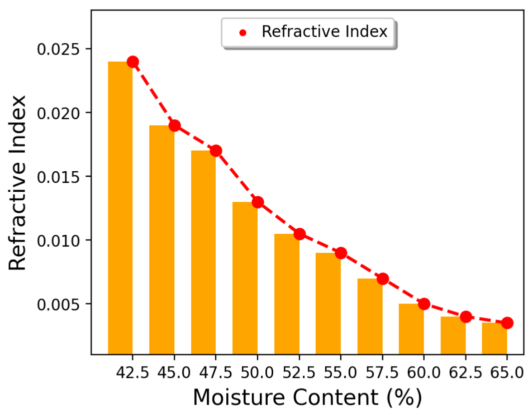

Fig. 4: Theoretical measurements of the refractive index of fruit.

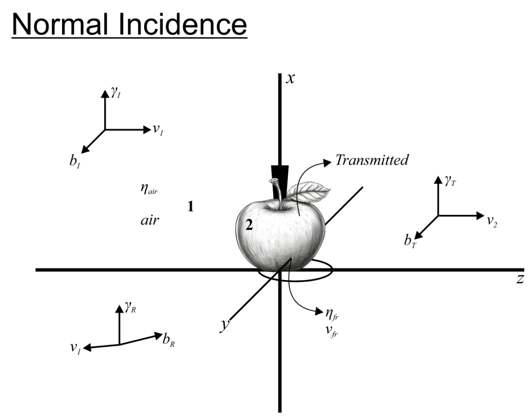

Fig. 6: Normal incidence scenario where radar waves strike the fruit perpendicularly for moisture level estimation.

V. Dual Incidence Moisture Estimation

This section examines the relationship between fruit moisture levels and radar signals, focusing on how the dielectric properties of fruit tissue change with moisture content. Moisture-rich fruits exhibit higher dielectric constants due to water's high permittivity, affecting both the amplitude and phase of the reflected signal (16). Key parameters such as the reflection coefficient, refractive index, attenuation factors, and fruit elasticity are crucial for accurate moisture detection.

First, we analyze the reflection coefficient, which measures the radar signal reflected by the fruit surface. As shown in Fig. 3, higher moisture content typically results in a lower reflection coefficient due to increased signal absorption, while lower moisture content leads to a higher reflection coefficient.

In Fig. 4, we discuss the refractive index, which increases as moisture decreases, as the fruit's solid components become more concentrated. We also examine fruit elasticity, which is directly related to moisture content. As fruit loses moisture, its turgor pressure decreases, causing the fruit to become softer and less elastic. Fig. 5 shows that higher moisture levels generally correlate with increased elasticity, making the fruit more flexible.

Finally, we introduce dual incidence moisture estimation, based on radar signal intensity at both normal and oblique incidences. This method yields a feature related solely to the electric properties of the fruit, providing a reliable indicator of moisture content and improving the precision of our model.

A. Signal Pre-processing

The raw mmWave signals the radar antennas receive cannot be directly used for fruit moisture detection due to bandwidth limitations, signal noise, and environmental interference. In indoor environments, RF signals often reflect off walls, ceilings, and moving objects, leading to multipath interference that complicates the signal. To address this, we use a Butterworth low-pass filter to remove noise and apply a range FFT to isolate the signal and extract the target zone. This process helps eliminate multipath interference and ensures a clearer signal for accurate moisture detection.

We then focus on the target zone, which corresponds to the area directly in front of the radar where the fruit is placed. This target zone contains the highest RSS values and the key discriminative features for moisture estimation. It is essential to closely examine this target zone for accurate moisture information. Fig. 8 presents the data after transformation via range-FFT. The peaks in the 0.2-meter range indicate the location of the detected object. This target zone holds critical features necessary for precise moisture estimation. Building on

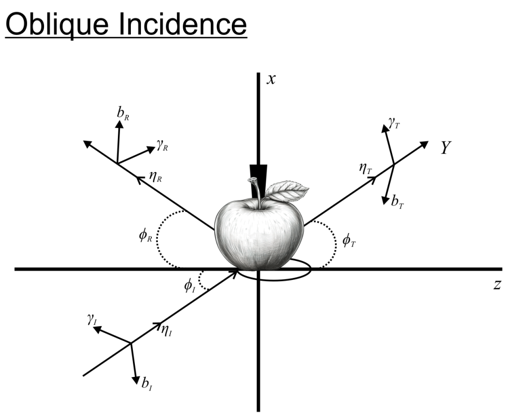

Fig. 7: Oblique incidence scenarios showing fruits positioned at various angles (0° to 180°, excluding 90°) relative to the mmWave radar for moisture level estimation.

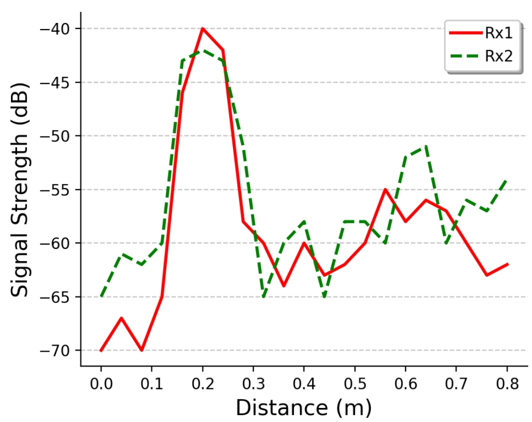

Fig. 8: Identification of target zone using FFT transformation.

existing research, we propose extracting moisture-dependent features from this peak zone. Specifically, we select consecutive samples in the 0.2-meter range with the highest signal strength values as data from the target zone. We then apply the dual incidence moisture estimation method to process these data, extracting crucial features such as reflection and location.

B. Fine-Grained Moisture Level Identification

When fruit dries, its refractive index changes significantly. This change is directly related to the reflection and transmission coefficients at both normal and oblique incidence. First, we directed mmWave at normal incidence as shown in Fig. 6 towards the fruit samples and calculated the reflection and transmission coefficients. As the fruit loses moisture, its refractive index and reflection coefficient increase. Electromagnetic waves are characterized by sinusoidal patterns and are denoted as $\eta = \frac{2\pi}{\lambda}$ and the angular frequency ω, where $\omega = \eta\nu$. An important property of electromagnetic waves is the equality of their parallel components when propagating across interfaces:

$$\text{i) } \varepsilon_{\text{air}}\gamma_{\text{air}}^{\perp} = \varepsilon_{\text{fr}}\gamma_{\text{fr}}^{\perp} \quad \text{and} \quad \text{ii) } \gamma_{\text{air}}^{\parallel} = \gamma_{\text{fr}}^{\parallel} \tag{6}$$

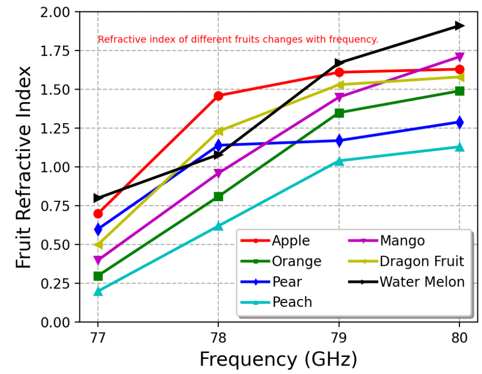

Fig. 9: Refractive index of different fruits as a function of frequency changes.

Here, ϵ_{air} represents the permittivity of air, $\gamma_{\text{air}}^{\perp}$ is the perpendicular component of the electric field in air, ϵ_{fr} denotes the permittivity of the fruit, and $\gamma_{\text{fr}}^{\perp}$ is the perpendicular component of the electric field in the fruit. The parallel components of the electric field are denoted as $\gamma_{\text{air}}^{\parallel}$ and $\gamma_{\text{fr}}^{\parallel}$ for air and the fruit, respectively. During normal incidence, there is no perpendicular component, so we disregard the first equation and use the second one:

$$\gamma_{\text{OI}} + \gamma_{\text{OR}} = \gamma_{\text{OT}} \tag{7}$$

Where γ_{OI} and γ_{OR} represent the complex amplitudes of the incident and reflected electric fields. The intensity of electromagnetic waves mainly depends on the amplitude of the electric field: $I = \frac{1}{2}\epsilon\nu\gamma_0^2$, where γ is the amplitude of the electric field. The fraction of incident energy that is reflected and transmitted can be found using the reflection coefficient r and transmission coefficient t:

$$r = \frac{I_R}{I_I} = \left(\frac{\gamma_{\text{OR}}}{\gamma_{\text{OI}}}\right)^2 = \left(\frac{n_{\text{air}} - n_{\text{fr}}}{n_{\text{fr}} + n_{\text{air}}}\right)^2 \tag{8}$$

$$t = \frac{I_T}{I_I} = \frac{\epsilon_{\text{fr}}\nu_{\text{fr}}}{\epsilon_{\text{air}}\nu_{\text{air}}}\left(\frac{\gamma_{\text{OT}}}{\gamma_{\text{OI}}}\right)^2 = \frac{4n_{\text{air}}n_{\text{fr}}}{(n_{\text{fr}} + n_{\text{air}})^2} \tag{9}$$

The reflection and transmission coefficients can be found using the refractive indexes of the two media. These equations allow us to measure the fraction of energy that is transmitted and reflected for the incident energy. As shown in Fig. 7, when radar waves strike the fruit surface at oblique angles, the reflected signals exhibit distinct characteristics due to changes in the propagation path and interaction with the fruit's internal structure. This involves analyzing the amplitude, phase, and polarization at different oblique angles. When the electromagnetic wave meets the boundary at an arbitrary angle ϕ_I, the reflection and transmission coefficients are given by:

$$r = \frac{I_R}{I_I} = \left(\frac{\gamma_{\text{OR}}}{\gamma_{\text{OI}}}\right)^2 = \left(\frac{X - Y}{X + Y}\right)^2 \tag{10}$$

$$t = \frac{I_T}{I_I} = \frac{\epsilon_{\text{fr}}\nu_{\text{fr}}}{\epsilon_{\text{air}}\nu_{\text{air}}}\left(\frac{\gamma_{\text{OT}}}{\gamma_{\text{OI}}}\right)^2 \frac{\cos\phi_T}{\cos\phi_I} = XY\left(\frac{2}{X + Y}\right)^2 \tag{11}$$

where $Y = \frac{\mu_{\text{air}} n_{\text{fr}}}{\mu_{\text{fr}} n_{\text{air}}}$ and $X \approx \frac{\cos\phi_T}{\cos\phi_I}$. Fig. 9 shows the transmission coefficient variation of different fruits, which is calculated by Eq. (11). Additionally, we proved that as the fruit loses moisture, its refractive index and reflection coefficient increase. These changes in reflection and transmission coefficients can be detected by a radar receiver, providing information about the freshness of the fruit.

C. Monitoring Moisture Level via Fruit Elasticity

One of the most important properties of solids is their elasticity, defined as the ratio of stress to strain. When a fruit dries, its elasticity noticeably changes because the turgor pressure within the fruit cells, which is maintained by water content, decreases. This affects the fruit's overall firmness and elasticity. As the water content reduces, cells become less turgid, leading to a reduction in turgor pressure. Consequently, fruits become more brittle, softer, or prone to wrinkling due to increased sugar and mineral content. These changes in elasticity can be used for moisture monitoring and can be determined through dielectric properties.

Dielectric property of fruit: Fruits have unique permittivity values due to their composition, moisture content, and structural characteristics. mmWave can detect variations in the permittivity as the fruit dries, allowing the measurement of reductions in elasticity. The dielectric property of fruit involves measuring the permittivity and loss factor. Complex permittivity indicates how much electric field energy a material can store, the real part of the mmWave signal represents stored energy while the imaginary part represents energy loss. The loss factor is the ratio of the imaginary part to the real part of the permittivity.

Using Maxwell's fourth equation in a medium, which involves electric displacement and magnetization, we derive:

$$\nabla \times \mathbf{h} = \sigma\gamma + bf\epsilon\gamma \tag{12}$$

where $\mathbf{h}$ is the magnetic induction, $\mathbf{b}$ is the magnetic field, ϵ is the permittivity of the material, γ is the electric field, and bf is the phasor operator ($b^2 = -1$). Simplifying, we get:

$$\nabla \times \mathbf{h} = bf\left(\frac{\sigma}{bf} + \epsilon\right)\gamma \tag{13}$$

$$\nabla \times \mathbf{h} = bf(\epsilon - \frac{\sigma}{bf})\gamma \tag{14}$$

Thus, the complex permittivity ϵ^* is:

$$\epsilon^* = \epsilon - \frac{\sigma}{f} \tag{15}$$

where ϵ is the real part and $\frac{\sigma}{f}$ is the imaginary part representing energy dissipation as heat due to charge movement within the material.

The elastic modulus E in terms of permittivity can be expressed as:

$$E = \frac{c}{a}\epsilon - \frac{cm}{a+d} \tag{16}$$

where a, b, c, d, and m are empirical constants determined through calibration at known moisture values in the lab by measuring the elastic modulus and permittivity.

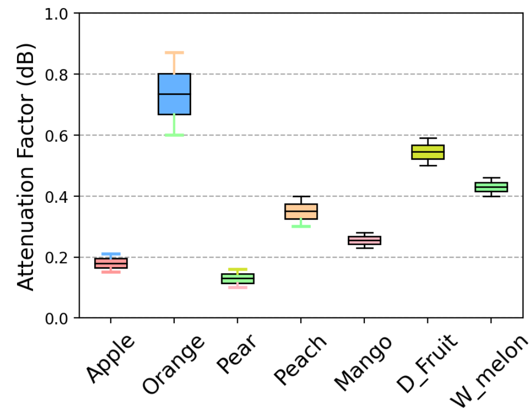

Fig. 10: Different fruits exhibit unique attenuation factors.

In mmFruit, the fruit is placed in front of the radar, which measures its dielectric properties by analyzing the reflected and transmitted signals. The radar system processes these signals to calculate the fruit's complex permittivity. Over time, changes in these parameters indicate changes in the dielectric properties. As the fruit dries, the real part of permittivity decreases, signaling a reduction in elasticity and an increase in the fruit's stiffness.

D. Eliminate Fruit Type Dependency

We calculate the attenuation factor to construct a feature independent of fruit type. By using the characteristic of complex permittivity as a function of frequency, we create a relative frequency response factor that does not depend on the fruit type. Eliminating the dependency on fruit type is challenging because the transport coefficient varies with the type of fruit, and it is inconvenient to pre-determine fruit type information. Fortunately, in the frequency domain, we observe that a medium's refractive index and complex permittivity change minimally with frequency, while the attenuation factor changes significantly.

To accurately identify fruit types using the mmFruit, we exploit the relationship between the attenuation factor and the complex permittivity of the fruit. Each fruit exhibits unique dielectric properties characterized by its complex permittivity, which consists of the real part (ϵ') and the imaginary part (ϵ''). By measuring the complex permittivity values using mmWave radar and calculating the attenuation factor as shown in Fig 10, we can create distinct profiles for different fruit types. The attenuation factor (α) is influenced by the material's complex permittivity and can be calculated using the formula (35):

$$\alpha = \omega\sqrt{\frac{\mu\epsilon'}{2}}\left(\sqrt{1 + \left(\frac{\epsilon''}{\epsilon'}\right)^2} - 1\right)^{1/2} \tag{17}$$

where ω is the angular frequency, and μ is the permeability of the material. By creating a comprehensive database of complex permittivity and attenuation factor profiles for various fruits, we can match the measured values of an unknown fruit to the profiles in the database, thus accurately identifying the

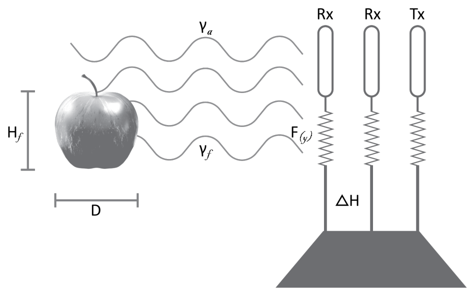

Fig. 11: Electric field distribution for different fruit sizes.

fruit type. This approach ensures precise fruit identification by leveraging the unique electromagnetic signatures of different fruits, allowing mmFruit to distinguish them effectively.

E. Eliminate Fruit Size Dependency

Eliminating fruit size is crucial for accurate moisture detection, as size variations can affect signal strength and lead to incorrect moisture estimations. By removing the size effect, measurements are solely dependent on moisture content, ensuring reliable results.

Fruit size affects signal strength: We configured one transmitting antenna and two receiving antennas to eliminate the size effect. Using fruits of varying heights, we analyzed signal strength at 77, 78, and 79 GHz. Our observations showed that signal strength varies with fruit size, impacting moisture estimation. To address this, we mapped the electric field around the receiving antennas and established a functional relationship between signal strength and size. Moving the transmitting antenna in the air helped eliminate the size influence on measurements.

Electric field distribution model: As shown in Fig. 11, the fruit's height is H_f and the antenna's height is H. When $H > H_f$, the signals near the antennas are transmitted through the fruit (γ_f) and the air (γ_a). The incident wave is a plane electromagnetic wave, so the electric fields γ_f and γ_a at frequency f are given by $\gamma_a = \Gamma_a z_a \gamma_a$ and $\gamma_f = \Gamma_f z_f \exp(BD)$, where D is the transmission distance in the fruit, B is the attenuation factor, z is the attenuation in air, and Γ_a and Γ_f are the transmission losses. With e_y as the unit vector in the vertical direction, the electric fields are expressed as $\gamma_a = e_y\gamma_a$ and $\gamma_f = e_y\gamma_f$. Let us define $\Omega = \frac{\Gamma_f z_f}{\Gamma_a z_a}$, thus we have $\gamma_f = \Omega \exp(-BD)\gamma_a$. The signal strength S_r^0 on the antenna is derived as:

$$S_r^0 = \int_0^{H_f} \gamma_f F(y)\,dy + \int_{H_f}^{H} \gamma_a F(y)\,dy \tag{18}$$

Using the previous relationship, this becomes:

$$S_r^0 = \Omega \exp(-BD)\gamma_a \int_0^{H_f} F(y)\,dy + \int_{H_f}^{H} F(y)\,dy \tag{19}$$

Where $F(y)$ represents the distribution of induced current on the antenna, which is related to the antenna and the signal wavelength.

Signal differential to eliminate size: Signals were collected at different fruit sizes. For every ΔH, the signal strength on the receiving antenna was collected to obtain a sequence $A = [a_0, a_1, \ldots, a_{n-1}]$:

$$a_j = S_r^j = \int_{j\Delta H}^{H_f} \gamma_f F(y)\,dy + \int_{H_f}^{H} \gamma_a F(y)\,dy$$

This simplifies to:

$$a_j = \Omega \exp(-BD)\gamma_a \int_{j\Delta H}^{H_f} F(y)\,dy + \gamma_a \int_{H_f}^{H} F(y)\,dy \tag{20}$$

The difference between consecutive elements is given by:

$$a_{j+1} - a_j = \Omega \exp(-BD)\gamma_a \int_{j\Delta H}^{(j+1)\Delta H} F(y)\,dy$$

By using the Riemann Sum, we get:

$$a_{j+1} - a_j = \Omega \exp(-BD)\gamma_a F(j\Delta H)\Delta H \tag{21}$$

Therefore:

$$\begin{aligned}
\Delta a &= a_{j+1} - a_j \\
\Delta a_{xr1} &= \Omega \exp(-BD_1)\gamma_a F(j\Delta H)\Delta H \\
\Delta a_{xr2} &= \Omega \exp(-BD_2)\gamma_a F(j\Delta H)\Delta H
\end{aligned} \tag{22}$$

The ratio is then:

$$\frac{\Delta a_{xr1}}{\Delta a_{xr2}} = \exp(-B\Delta D) \tag{23}$$

where $\Delta D = D_1 - D_2$. Eq: (23) is independent of the size/height of the fruit.

VI. mmFruit System Design

The workflow of mmFruit as shown in Fig. 12, involves four steps. First, the mmWave radar transmits signals toward the target fruit and collects the reflected signals. Next, signal pre-processing which involves signal refinement, noise cancellation, extracting range estimations, and identifying range bins, where the fruit is placed. Then, reflection features are extracted across three different mmWave frequencies based on the dual incidence moisture estimation model. Finally, these features from multiple range bins are fed into a spatially invariant network (SpI-Net) to estimate the moisture level of fruits. The main steps of mmFruit are:

- **Different frequencies features:** mmFruit employs an innovative dual incidence model to capture reflections across various frequencies during each chirp, enhancing its ability to discern detailed features of fruit moisture levels. The process begins by dividing the collected samples, taken at three different frequencies (77 to 79 GHz), into three channels based on their starting and ending frequencies. Reflection features from both normal

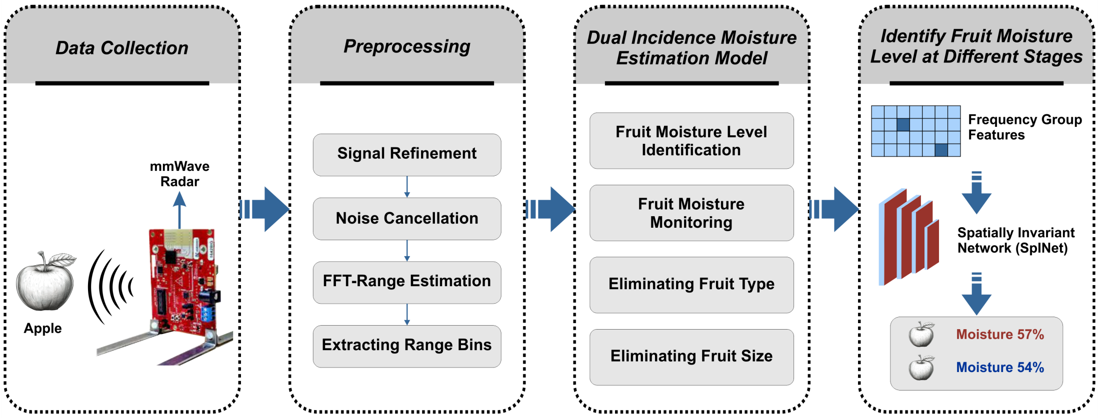

Fig. 12: Overview of the mmFruit Model

and oblique incidences are individually extracted and consolidated into distinct channels and then by extracting reflection coefficient, fruit refractive index, complex permittivity, and fruit elasticity from each channel, which effectively monitor and represent fruit moisture level.

- **Identifying fruit moisture level at different range bins using SpI-Net:** We developed a customized neural network called SpI-Net to process features extracted from different range bins and frequencies. SpI-Net incorporates a spatially invariant feature extraction module that automatically identifies moisture-dependent features across various locations. These features are subsequently inputted into a moisture prediction module for content inference. Through training on diverse datasets collected from multiple positions and angles, SpI-Net learns to consistently extract moisture-dependent features, enabling accurate moisture identification across different locations.

A. *Different Frequencies Unique Features*

To explore the potential of mmWave radar for fine-grained fruit moisture level sensing, we leveraged the unique interaction of electromagnetic (EM) waves with dielectric materials across different frequencies. Specifically, we employed three distinct frequencies (77 to 79 GHz). Inspired by the fact that dielectric properties (39), such as complex permittivity, reflection coefficient, and fruit elasticity vary with radio frequency, we hypothesized that the reflection characteristics of fruits would also differ across different mmWave frequencies, providing valuable insights about moisture levels. The relationship between permittivity (ψ) and electromagnetic frequency (f) can be described using the Double Debye equation (17), which is particularly effective at high frequencies.

The Double Debye equation is expressed as:

$$\psi = \psi' - j\psi'' = \psi_\infty + \frac{\psi_s - \psi_1}{1 + j2\pi f\tau_1} + \frac{\psi_1 - \psi_\infty}{1 + j2\pi f\tau_2} \qquad (24)$$

where ψ' and ψ'' are the real and imaginary parts of the permittivity, representing the stored energy and energy loss within the material, respectively. ψ_∞ is the permittivity at infinite frequency, while ψ_s is the permittivity at static (zero) frequency. ψ_1 denotes the permittivity at an intermediate frequency. The parameters τ_1 and τ_2 are the relaxation time constants associated with the transitions from static to intermediate, and intermediate to infinite permittivity, respectively. Additionally, j is the imaginary unit, indicating the phase shift between the electric field and the polarization of the material.

$$\psi' = \psi_\infty + \frac{\psi_s - \psi_1}{1 + (2\pi f\tau_1)^2} + \frac{\psi_1 - \psi_\infty}{1 + (2\pi f\tau_2)^2} \qquad (25)$$

$$\psi'' = \left(\frac{\psi_s - \psi_1}{1 + (2\pi f\tau_1)^2}\right) \cdot 2\pi f\tau_1 + \left(\frac{\psi_1 - \psi_\infty}{1 + (2\pi f\tau_2)^2}\right) \cdot 2\pi f\tau_2 \qquad (26)$$

According to these equations, the permittivity of the same moisture content changes with the frequency of the signals used to measure it. Measurement results from existing literature confirm that both ψ' and ψ'' decrease as the frequency increases (40), (30). We can obtain multiple reflection features using mmWave signals at different frequencies by applying these equations. We then extract these features to verify their effectiveness in identifying finer-grained moisture content. This approach enhances the sensitivity and accuracy of moisture detection and demonstrates the effectiveness of multi-frequency analysis in fruit moisture sensing using mmWave radar.

B. *Frequency Group Features Extraction*

mmWave operates within the 77 to 81 GHz frequency range, providing high-resolution perception. We utilize this broad range to extract reflection characteristics of fruit, focusing on accurate moisture measurement across frequencies. The FMCW mmWave radar's starting frequency was adjusted to capture reflection features at various mmWave frequencies, dividing the samples into three channels (77-79 GHz) (41). Features were extracted from different range bins using Range-FFT for each channel, and then combined into a single group for spatial invariant feature extraction.

For moisture analysis, we used a sliding window of data samples collected during one chirp from 77-79 GHz. Range-FFT was applied to extract the refractive index, reflection coefficient, complex permittivity, and elasticity from the target

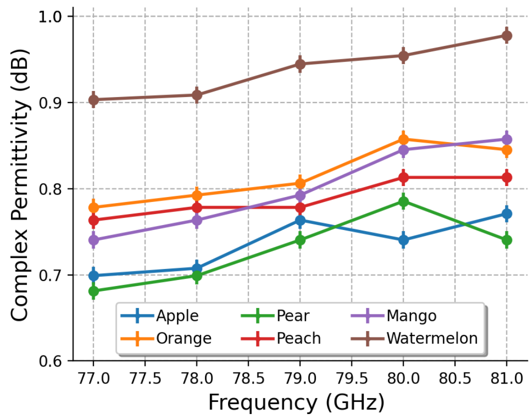

Fig. 13: Measurement of fruit complex permittivity at different mmWave frequencies across varying moisture levels.

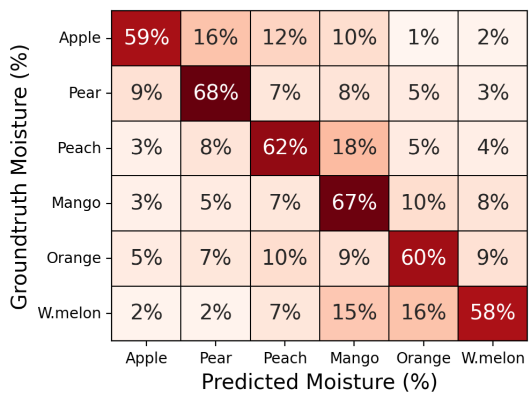

Fig. 14: Evaluation of mmFruit's accuracy using a state-of-the-art sensing method, achieving an average accuracy of 62.3%.

zone and generating 4-channel features. This enabled differentiation of fruits with moisture levels ranging from 45% to 63%. As shown in Fig. 13, frequency shifts are crucial for creating distinct features. Dividing the spectrum into more channels increases reflection diversity but adds computational complexity. Ablation studies showed that three channels were optimal, balancing inter-channel overlap and range resolution, set at 3.8 cm with a 4 GHz bandwidth per channel.

C. mmFruit using the state-of-the-art sensing method

This section evaluates our moisture estimation method compared to Wi-Fruit (16). Wi-Fruit struggles to distinguish moisture levels across different range bins, prompting us to develop a data-driven approach using a custom CNN-ANN model to improve moisture detection accuracy by reducing location-based interference. We collected data from six fruits with varying moisture levels across distances from 15 cm to 30 cm, gathering 1,500 samples per position for training, and repeated the process at five additional positions to generate a test set. In total, we obtained 12,860 training samples and 5,480 testing samples.

Using Wi-Fruit's method, which estimates moisture through relative permittivity via RSS and phase features, we trained our model. Test results, shown in Fig. 14, reveal an average accuracy of 62.3% in identifying moisture levels. Compared to Wi-Fruit's RMSE of 0.319, this reduced accuracy demonstrates mmWave sensing's sensitivity to location changes, likely due to its shorter wavelength. Wi-Fruit employs a lightweight ANN to learn from data across various positions, reducing interference from minor displacements. However, accuracy significantly declines with larger displacements (e.g., 30 cm) due to the ANN's limited three-layer structure, which struggles to handle performance consistency across wider displacements. To address this, we introduce the Spatially Invariant Network (SpI-Net), which effectively manages target displacements and enhances moisture estimation accuracy.

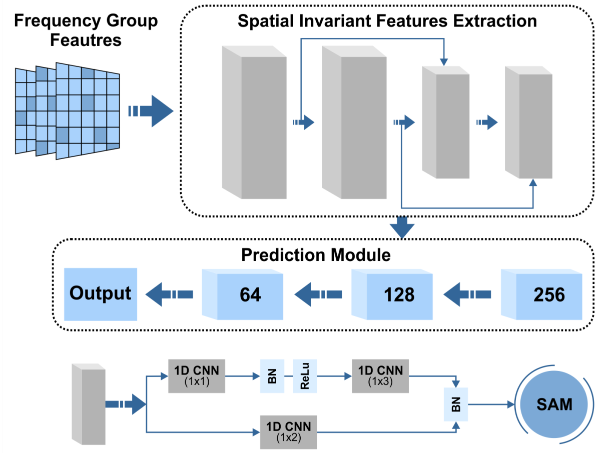

Fig. 15: SpI-Net Structure.

VII. Overview of SpI-Net

The structure of SpI-Net is shown in Fig. 15, consisting of two main modules: the spatial invariant feature extraction module and the fruit moisture level prediction module. In the feature extraction module, one-dimensional convolution layers is used to extract features that remain consistent across different ranges of target fruit positions. By downsampling these features with max pooling, SpI-Net ensures that reflection characteristics are preserved even when fruits are located in various locations. This approach efficiently captures moisture-related features locally and globally (42). These extracted features are then fed into the moisture level prediction module, which employs three fully connected layers to predict moisture levels. SpI-Net utilizes residual convolution for feature extraction to achieve spatial invariance globally, a method proven effective in image processing (43). In Fig.16, the Spatial Attention Model (SAM) is illustrated to effectively capture reflection features with varying fruit moisture levels across different range bins. This involves multi-head attention (44), which calculates attention scores and weights among elements in the input sequence to capture relationships and dependencies, aided by batch normalization during training. As a result, SpI-Net employs one-dimensional residual convolutional layers instead of the lightweight ANN model used in Wi-Fruit.

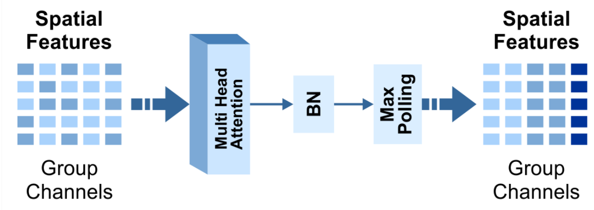

Fig. 16: Spatial Attention Module (SAM).

A. SpI-Net Input Data

To collect our data, we gathered samples using different frequencies and processed them with range-FFT (45) to capture signals from varying distances. These signals were combined to extract important reflection features. Unlike Wi-Fruit, which focuses on extracting permittivity features from specific fruit range bins, SpI-Net takes a broader approach and uses features from multiple range bins to cover a wider area. For instance, it considers range bins from 15 cm to 30 cm, accommodating different radar-target distances encountered in real-world situations. From both normal and oblique angles, we extract four key features based on the dual-incidence moisture estimation model: the signal reflection coefficient, fruit refractive index, complex permittivity, and fruit elasticity. These features serve as inputs to the SpI-Net, offering comprehensive reflection and moisture information about the fruits.

B. SpI-Net Structure

The Spatial Invariant feature extraction module consists of four primary blocks. As shown in Fig. 15 each block groups and downsamples features across multiple range bins using a convolutional layer with a stride of 2. The second, third, and fourth blocks incorporate residual connections to capture global invariant features. Each block has two branches: a main branch and a residual branch. The main branch applies a 1-dimensional convolution (Conv1d) layer with a 1×1 kernel to capture local features within a range bin, followed by a Conv1d layer with a 1×2 kernel to enhance feature detection across adjacent range bins. The residual branch includes a Conv1d layer with a 1×3 kernel to align the input and output feature maps, providing a shortcut connection to prevent gradient loss during training. Each Conv1d layer integrates batch normalization and ReLU activation to improve feature extraction through non-linear transformations.

Within each block, a Spatial Attention Module (SAM) based on multi-head attention focuses on the most informative features across channels. As shown in Fig. 16, SAM begins by selecting representative features from each channel through max-pooling across bins, then applies non-linear transformations to generate channel-wise attention weights using multi-head attention, incorporating normalization, dropout, and activation. These refined features feed into the moisture level prediction module, which flattens the 2-dimensional features into a 1-dimensional vector and uses three fully connected layers to output moisture level probabilities. The first two layers use ReLU activation, enhancing robustness in moisture prediction.

VIII. Evaluation

This section evaluates the performance of mmFruit through a series of experiments. We discuss the hardware and software implementation, describe the experimental setup for fruit moisture categorization, and analyze mmFruit's estimation accuracy.

A. Implementation

- **Hardware Requirements:** The mmFruit prototype uses a COTS FMCW mmWave radar, the TI-IWR1443 (46), connected via USB to a computer. The radar operates between 77 GHz and 81 GHz. The algorithms are implemented in Jupyter Notebook on a MacBook with an Intel Core i5 CPU and 16 GB memory, communicating with the DCA1000EVM through Ethernet. The trained mmFruit model can be deployed on various mmWave-supported devices, making it adaptable for daily applications.
- **mmWave Radar Setup:** A single transmitting-receiving antenna measures fruit moisture levels. Each radar frame contains 128 chirps sweeping from 77 GHz to 79 GHz. With an ADC sample rate of 256 MHz and a chirp duration of 30 microseconds, each frame collects data over 5 ms. The IF samples are stored in a .bin file for signal processing and inference via the SpI-Net model.
- **Model Training:** SpI-Net's feature extraction module consists of four convolutional blocks with a multi-head attention mechanism, reducing channels to 32 before rescaling. Prediction is achieved through three fully connected layers (output sizes of 256, 128, and 64). The model uses softmax cross-entropy loss with the Adam optimizer and a batch size of 16, starting with a learning rate of 0.002, which decreases adaptively. Training halts after three learning rate reductions or 120 epochs.

B. Experimental Setup

The experiment categorizes fruit types based on moisture levels, using penetrometers to measure ground truth moisture for each type. We then use mmWave radar to capture reflections and estimate moisture content. To validate mmFruit's sensing capability, we collected seven fruit types with thin and thick pericarp from a local market. Stored in a cotton box to simulate natural degradation over a month, this diverse collection included fresh, rotted, and low-quality samples.

Our moisture content estimation setup evaluates three scenarios:

- Detection across varied moisture levels: Seven fruit types with moisture levels between 45% and 65% were selected, covering a broad moisture range to ensure detection reliability.
- Identification of similar moisture content: Fruits with small moisture variations (0% to 7%) were tested, posing a challenge due to their similar appearance and moisture levels.
- Regular monitoring: Fruit moisture levels were tracked over 30 days to assess sensor accuracy and degradation detection over time during storage.

TABLE II: Details of data collection.

Parameter	Details
Fruit Moisture	24 fruits of different moisture contents
Training Samples	16,000 for each frequency category
Testing Samples	8,000 for each frequency category
Range Bins	0.2 - 1.0 meters
Range Angles	0-180 degrees

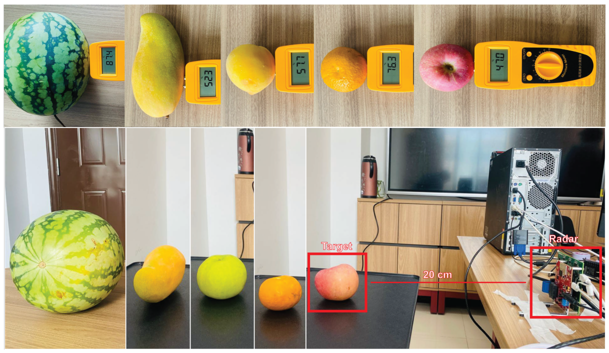

Fig. 17: Experimental setup for mmFruit and ground truth moisture estimation using commercial off-the-shelf (COTS) devices.

1) Ground Truth Collection

To accurately determine the moisture values for each fruit, we used COTS devices as shown in Fig. 17. We employed the SmartSensor AR991 and Jacks JK-100R penetrometers, each with an accuracy of 0.1%. Before each measurement, the refractometer mirror and penetrometer probe were calibrated using de-ionized water and then air-dried.

2) Data Collection

To evaluate mmFruit's performance, we used a mmWave device to collect moisture data from a variety of fruits with both thin and thick pericarps, as shown in Fig. 17. We captured mmWave signals at three frequencies (77-79 GHz) from fruits with different moisture levels, positioning each fruit at various distances and angles relative to the radar. The setup involved placing the device on a table and positioning the fruits at distances ranging from 0.2 to 1.0 meters, with five adjustments per fruit. For each position, 200 samples were collected per frequency at a rate of 20 frames per chirp, resulting in a total of 16,000 training samples across all distances and frequencies. For the test set, we collected 8,000 samples from 10 additional fruits, positioned at new locations within the training range.

As summarized in Tab. II, our dataset comprises 24,000 samples from 24 fruits, covering moisture levels between 45% and 65%. This dataset was essential for evaluating mmFruit's accuracy across different distances and angles. The experiments were conducted on a wooden table in a temperature-controlled room, with additional samples taken from various fruit types and sizes under diverse environmental conditions.

IX. mmFruit Overall Performance

We evaluate mmFruit through multiple experiments designed to monitor fruit moisture, identify fruit types and sizes, and detect minor and major moisture variations. Specifically,

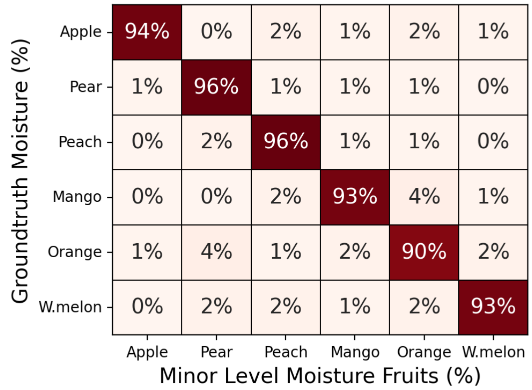

Fig. 18: Performance evaluation of mmFruit in identifying minor moisture level differences ranging from 0% to 7%.

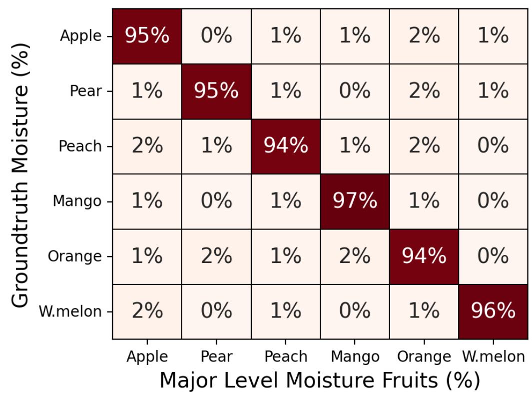

Fig. 19: Performance evaluation of mmFruit for identifying major moisture levels changes within the 44% to 65% range.

we focused on monitoring moisture levels with minor variations from 0% to 7% and major moisture levels from 45% to 65%. The outcomes of these experiments provided valuable insights:

- **Minor level changes in fruit moisture:** Our focus was on accurately distinguishing minor differences in moisture levels among fruits. mmFruit demonstrates excellent performance, achieving an average accuracy of 93.6% in classifying fruits with minor moisture level variations ranging from 0% to 7%, as illustrated in Fig. 18. This level of precision is particularly crucial in applications where even slight changes in moisture level can significantly influence fruit quality, shelf life, and overall consumption. By effectively identifying these subtle differences, our system facilitates precise sorting and grading of fruits, ensuring consistent quality standards and enhancing consumer satisfaction. Furthermore, the insights gained from analyzing these moisture variations are invaluable for optimizing post-harvest processes, thereby improving the efficiency and effectiveness of the entire production chain.
- **Major level changes in fruit moisture:** In the second experiment, mmFruit's ability to precisely identify different moisture content levels based on ground truth

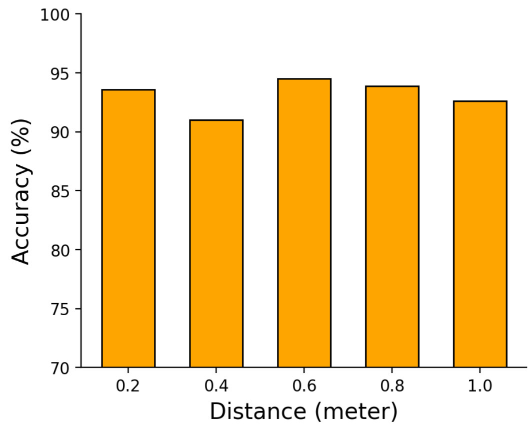

Fig. 20: Performance evaluation of mmFruit in identifying moisture levels at varying distances.

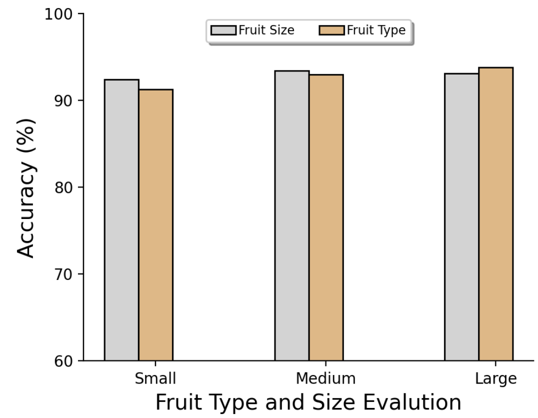

Fig. 21: Performance evaluation of mmFruit for identifying different fruit types and sizes.

values was evaluated. As depicted in Fig. 19, the system demonstrates a remarkable average accuracy of 95.1% in discerning moisture levels ranging from 44% to 63%. This robust performance highlights mmFruit's capability across a broad spectrum of moisture detection. It contributes significantly to consumer safety by identifying fruits with higher moisture levels that are prone to mold and bacterial growth. Moreover, it plays a crucial role in ensuring the quality of the product before it reaches the market, thereby enhancing food safety standards.

TABLE III: Performance evaluation of regular fruit moisture monitoring using RMSE.

Fruit Type	RMSE
Apple	0.229
Orange	0.270
Pear	0.263
Peach	0.201
Mango	0.362
Dragon Fruit	0.283
Watermelon	0.330
Overall RMSE	**0.276**

- **Daily fruit moisture monitoring:** To regularly monitor fruit moisture over time, we collected radar signals from each fruit type continuously for 15 days. The estimation accuracy for each fruit type, represented by RMSE values, is shown in Tab. III. The results indicate that the estimation accuracy for most fruit types remains high throughout the week, with an overall RMSE of 0.276. This demonstrates that our method can be applied at any time and provides accurate results on-site.
- **Fruit moisture sensing at various distances:** The robustness of mmFruit Sensing across multiple locations is demonstrated in Fig. 20, the system demonstrates an average accuracy of 93.12%. We evaluate the robustness of mmFruit by testing moisture sensing at varying distances and angles of rotation. Despite changes in the fruit's position, our model consistently provides precise moisture estimations. This performance highlights the system's reliability and robustness across multiple distances and random rotations, making mmFruit suitable for diverse mobile applications in real-world scenarios.
- **Fruit type identification:** We evaluated mmFruit for identifying different fruit types by using the fruit attenuation factor, which is unique to each fruit. As shown in Fig. 21, the accuracy for each fruit type shows that our model can effectively identify fruits without needing visual information. By using the fruit attenuation factor, mmFruit takes advantage of the electromagnetic properties of the fruits, resulting in reliable classification.
- **Fruit size identification:** We evaluated the mmFruit model for identifying different fruit sizes by dividing the dataset into three categories: small, medium, and large fruits. The model was tested using fruits of various sizes, and we developed a differential model employing two receiving antennas to enhance size detection accuracy. Fig. 21 illustrates the accuracy of the model for each size category, showing that mmFruit can effectively identify fruit sizes. This capability is particularly valuable for sorting fruits based on size.

A. Comparison of mmFruit with State-of-the-art methods

We compare mmFruit with two advanced methods for moisture identification: Wi-Fruit (16) and Moisture Content Identification Using Terahertz (14). Wi-Fruit employs a dual-quotient, model-based CSI preprocessing technique to mitigate interference from target distance, aiming to remove the dependency on fruit structure in moisture estimation across various types of fruit. In contrast, the Terahertz (THz) method utilizes THz frequencies to estimate moisture content. We applied both methods to our dataset, following their methodologies to extract features such as the relative permittivity of fruits and other descriptive characteristics. We also implemented their deep learning models for training and testing to evaluate their performance. While Wi-Fruit uses a WiFi-based approach for feature extraction, focusing on distance-independent methods in both time and frequency domains and leveraging amplitude

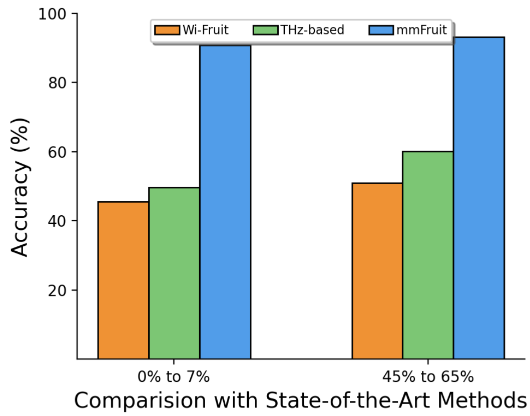

Fig. 22: Comparison of mmFruit with state-of-the-art methods.

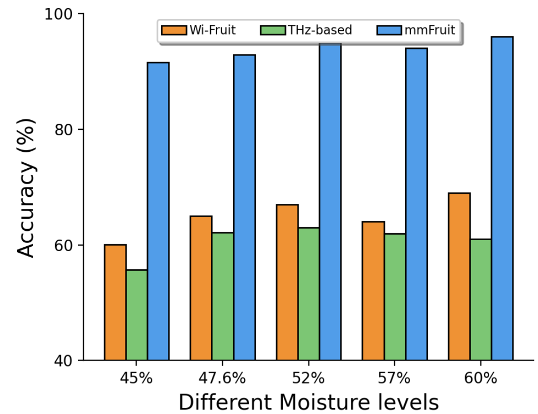

Fig. 23: Presents the binary classification average accuracy for fruits with high and low moisture content when the radar-target angle and distance vary.

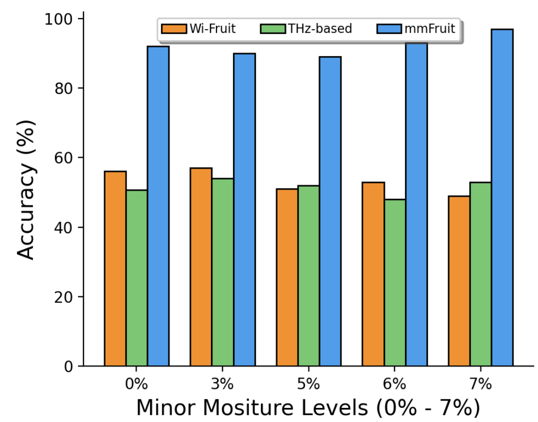

Fig. 24: Illustrates the accuracy of identifying fruits with similar moisture content, specifically with a moisture difference of 0% to 7%.

and phase measurements within a 20 cm range, we employed a single mmWave receiving antenna to compute feature vectors for each sample. We then used SpI-Net to classify the moisture levels of the fruit.

The proposed SPI-Net outperforms existing methods due to its use of a targeted set of features based on the physical properties of fruits, such as refractive index, elasticity, and attenuation factor, which directly correlate with moisture content. In contrast, Wi-Fruit and the THz method include all available features, some of which may introduce irrelevant or noisy data, reducing accuracy. Additionally, SPI-Net employs a Spatial Attention Module (SAM) to select the most relevant features for moisture estimation, focusing the model on key physical properties. Unlike other methods that do not prioritize features, the SAM module enhances SPI-Net's adaptability and robustness across different fruit types and moisture conditions, leading to superior accuracy and more reliable moisture detection.

- Fine-grained moisture estimation with varying radar-target displacement was examined. In Fig. 22, both Wi-Fruit and the THz-based methods for moisture level estimation struggled to achieve precise results under significant changes in target distance and angle. Wi-Fruit attained average accuracies of 45.6% and 51.0% on our datasets, while the THz-based method achieved 49.7% and 60.1%. In contrast, mmFruit demonstrated an accuracy, exceeding 90.8% and 93.2%. To assess the limitations of these methods, we conducted separate tests to evaluate their capabilities for fine-grained identification and the effects of radar-target displacement.
- We assessed coarse-grained moisture estimation from 0% to 7% compared to levels between 45% and 65%, varying radar-target distances and angles. We conducted binary classification distinguishing high moisture (65%) from lower levels. Results in Fig. 23 reveal that Wi-Fruit and THz-based methods achieved over 62.8% accuracy in distinguishing 45% to 60% moisture differences under varying conditions. However, Fig. 24 shows their accuracy dropped below 52.39% for 0% to 7% moisture differences, indicating significant impairment by radar-target changes. In contrast, mmFruit demonstrated robust performance against displacement, maintaining over 93% accuracy using SpI-Net.

B. *Micro-benchmark Experiments*

In this section, we assess our innovations' strengths. Firstly, we enhance sensitivity and precision in moisture detection by leveraging multi-frequency features. Secondly, SpI-Net's unique architecture uses shared convolutional kernels and residual connections to robustly identify moisture under varying radar conditions. Together, these innovations enhance mmFruit's reliability and performance in the non-destructive moisture assessment of fruits.

- **Impact of different frequency features:** To validate the advantages of using different frequency reflection features for precise moisture estimation, we segmented mmWave signals into varying numbers of frequency channels to extract SpI-Net features. Specifically, we utilized signals from 77, 78, and 79 GHz, dividing them into three frequency channels with 3.93 GHz bandwidth each. As shown in Fig. 25 illustrates the average accuracy in

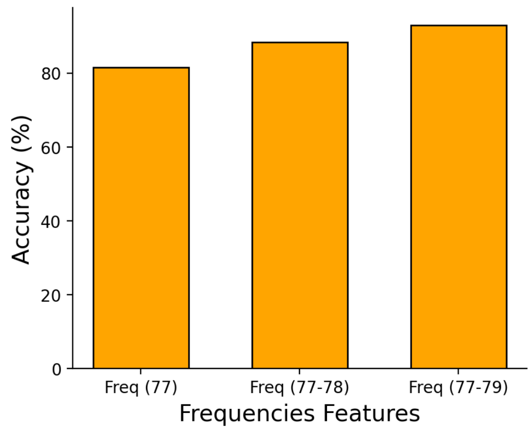

Fig. 25: Illustrates the performance of dividing the mmWave signal into varying numbers of frequency channels.

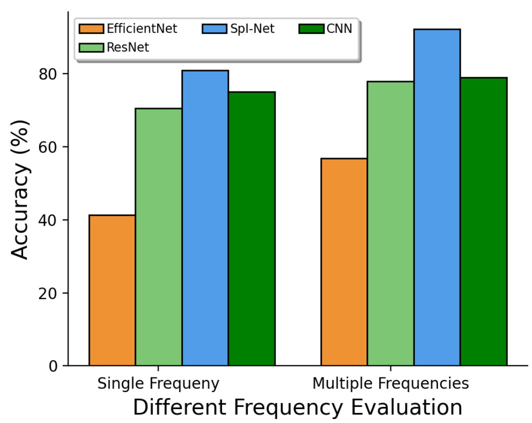

Fig. 26: Comparison of SpI-Net with CNN, EfficientNet (47) and ResNet (48) for identifying fruits with moisture content ranging from 45% to 65%.

identifying moisture content between 45% and 65%. Using features from a single frequency yielded 81.6% accuracy. Increasing channels to two improved accuracy to 88.3%, attributed to additional reflection features. Further increasing to three channels resulted in 93% accuracy, getting benefit from increased feature overlap, which reduces differences across channels. To maintain adequate range resolution, we maintained the sample count per channel without reduction. Therefore, we recommend dividing 77 GHz to 79 GHz mmWave signals into three channels, each with approximately 4 GHz bandwidth.

- **SpI-Net comparison with existing neural models** To evaluate our novel SpI-Net, we compared it with three neural models: ResNet-50 (48), EfficientNet (47), and a state-of-the-art CNN model. EfficientNet manages different range bin reflections and utilizes fully connected layers to mitigate displacement interference. ResNet, a renowned convolutional neural network, was adapted by replacing its 2D convolutions with 1D convolutions to suit our data structure. Additionally, the CNN model used in this comparison employed three convolutional layers with batch normalization and pooling, followed by three fully connected layers. Fig. 26 displays their performance in distinguishing nine fruits with moisture content ranging from 45% to 65%.
We compared all models based on single-frequency features, which were extracted using the 77 GHz band, and multiple-frequency features, which were extracted using the 77-79 GHz range. In contrast, SpI-Net achieved significantly higher accuracies with both single and multiple-frequency features. When incorporating multi-frequency features, SpI-Net achieved an average accuracy of 92.3%, surpassing CNN, EfficientNet, and ResNet. This performance is attributed to SpI-Net's specialized architecture, which minimizes information loss by reducing excessive feature pooling and downsampling. Additionally, the inclusion of residual connections and SAM modules in each block enhances the network's capability to capture and utilize features crucial for moisture content estimation.

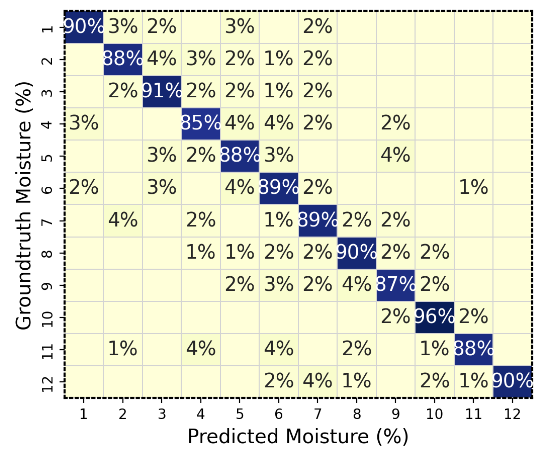

Fig. 27: Confusion matrix for classifying 12 fruit moisture levels.

C. Case Study I: Fruit Classification Based on Moisture Level

mmFruit offers a cost-effective way for consumers to select high-quality fruits based on moisture levels, rather than relying on potentially misleading visual appearance. Traditionally, consumers choose fruits based on their look, sometimes picking visually appealing but tasteless ones. mmFruit categorizes fruits based on internal quality, measured by moisture.

To validate mmFruit, we labeled fruits with various moisture levels, collecting mmWave samples from each type and measuring ground truth moisture levels using a penetrometer. After range-FFT preprocessing, the reflected mmWave signals were used to train a SpI-Net classifier for moisture estimation and internal quality identification. As shown in Fig. 27, the classification results showed that mmFruit achieved 91% accuracy in classifying internal quality based on moisture levels. This demonstrates mmFruit's ability to provide reliable information for consumers, improving fruit quality assessment and enabling retailers to optimize pricing and profitability.

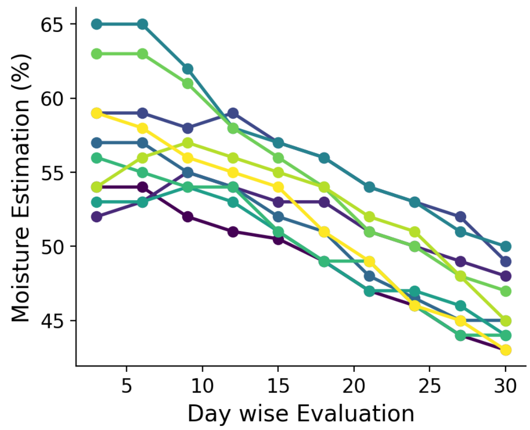

Fig. 28: Apple moisture level degradation over time.

D. Case Study II: Apple Shelf Life and Storage

mmFruit's non-destructive capabilities enable continuous monitoring of moisture levels as fruits deteriorate at room temperature. In this study, we tracked the moisture levels of twelve apples daily over a month, stored at 23°C, using visible wrinkles or spoilage as the reference point.

Most apples showed the sharpest moisture decline from the day of purchase to the reference day, typically within three days. We averaged the moisture values from the reference day and the following three days, as shown in Fig. 28. Key observations included moisture decline as fruit skins decayed, occasional moisture increases before decreases due to ripening, and some apples showing minimal moisture drop despite visible spoilage. These findings suggest varying storage periods for apples, with some requiring immediate consumption and others being suitable for longer storage based on internal features estimated by mmFruit. This demonstrates mmFruit's value in predicting internal quality and offering tailored storage recommendations for consumers and retailers.

X. Limitations and Future Work

The limitation of the mmFruit is the limited penetration depth of mmWave signals, especially in fruits with dense or thick outer layers. This constraint affects the accuracy of internal moisture content measurements, as mmWave signals may only provide information about the outer regions of larger or denser fruits, such as avocados or coconuts. To address this issue, future work should focus on developing enhanced signal processing techniques or alternative imaging methods that improve penetration depth. Exploring multi-frequency or multi-modal sensing approaches could offer a more comprehensive assessment of moisture content in fruits with dense outer layers. Also, mmWave radar generally requires a higher initial investment than standard Wi-Fi-based systems due to specialized components and higher frequency operation. This added cost could impact widespread adoption, particularly for smaller-scale or budget-constrained agricultural operations.

Another limitation is the tradeoff between normal and oblique incidence of mmWave signals, which varies by fruit type and size. For instance, the refractive ratio of fruits like apples remains relatively constant across incidence angles, while fruits such as watermelon exhibit significant sensitivity to the angle of incidence. Future research should aim to develop adaptive sensing strategies that account for these variations. Implementing angle-specific calibration techniques and optimizing incidence angles based on fruit characteristics will enhance the accuracy of moisture detection and ensure reliable measurements across different fruit types and sizes.

XI. Conclusion

In this study, we introduce mmFruit, a novel system utilizing a dual-incidence moisture estimation model based on 77GHz mmWave radar to accurately distinguish varying moisture contents in fruits. By leveraging unique radar reflections, refractive indices, fruit complex permittivity with attenuation factors, and fruit elasticity, it employs SpI-Net, a custom-designed convolutional neural network, for precise and robust moisture identification. Experimental validation demonstrates mmFruit's capability to monitor and estimate fruit moisture levels, discerning moisture content differences of 0%-7% and 45%-65% under diverse conditions, including random displacement and rotation. Additionally, our case studies track moisture levels over several days, highlighting mmFruit's effectiveness in monitoring and detecting moisture changes. The case studies further validate the practical applicability in real-world scenarios, such as storage and shelf-life monitoring. This research underscores mmFruit's potential in enhancing fruit quality assessment and shelf-life management, offering a reliable tool for agricultural and food industry applications.

References

[1] G. B. Seymour, J. E. Taylor, and G. A. Tucker, *Biochemistry of fruit ripening*. Springer Science & Business Media, 2012.

[2] A. A. Kader, "Fruit maturity, ripening, and quality relationships," in *International Symposium Effect of Pre-& Postharvest factors in Fruit Storage 485*, 1997, pp. 203–208.

[3] K. Tu, B. Nicolaı, and J. De Baerdemaeker, "Effects of relative humidity on apple quality under simulated shelf temperature storage," *Scientia Horticulturae*, vol. 85, no. 3, pp. 217–229, 2000.

[4] N. Sharma, S. Jandaik, S. Kumar, M. Chitkara, and I. S. Sandhu, "Synthesis, characterisation and antimicrobial activity of manganese-and iron-doped zinc oxide nanoparticles," *Journal of Experimental Nanoscience*, vol. 11, no. 1, pp. 54–71, 2016.

[5] R. Fouladi-Fard, R. Aali, S. Mohammadi-Aghdam, and S. Mortazavi-derazkola, "The surface modification of spherical zno with ag nanoparticles: A novel agent, biogenic synthesis, catalytic and antibacterial activities," *Arabian Journal of Chemistry*, vol. 15, no. 3, p. 103658, 2022.

[6] B. M. Nicolai, K. Beullens, E. Bobelyn, A. Peirs, W. Saeys, K. I. Theron, and J. Lammertyn, "Nondestructive measurement of fruit and vegetable quality by means

of nir spectroscopy: A review," *Postharvest biology and technology*, vol. 46, no. 2, pp. 99–118, 2007.

[7] N. Khalid, A. Abdullah, S. Shukor, F. S. AS, H. Mansor, and N. Dalila, "Non-destructive technique based on specific gravity for post-harvest mangifera indica l. cultivar maturity," in *2017 Asia Modelling Symposium (AMS)*. IEEE, 2017, pp. 113–117.

[8] STELZNER, "Fruit penetrometer," https://pronova.de/en/products/agricultural-measuring/fruit-analysis/804, accessed: 2024-11-06.

[9] Jacks, "Jk-100r penetrometer moisture analyzer," https://www.chem17.com/product/detail/28186372.html, accessed: 2024-11-06.

[10] Yamato, "Adp-31 vacuum oven," https://www.idealvac.com/files/brochures/yamatovacuumovenadp21_31.pdf, accessed: 2024-11-06.

[11] M. Ecarnot, P. Baczyk, L. Tessarotto, and C. Chervin, "Rapid phenotyping of the tomato fruit model, micro-tom, with a portable vis–nir spectrometer," *Plant physiology and biochemistry*, vol. 70, pp. 159–163, 2013.

[12] J. F. I. Nturambirwe, H. H. Nieuwoudt, W. J. Perold, and U. L. Opara, "Non-destructive measurement of internal quality of apple fruit by a contactless nir spectrometer with genetic algorithm model optimization," *Scientific African*, vol. 3, p. e00051, 2019.

[13] Felix, "F-750," https://felixinstruments.com/food-science-instruments/portable-nir-analyzers/f-750-produce-quality-meter/, accessed: 2024-11-06.

[14] A. Ren, A. Zahid, A. Zoha, S. A. Shah, M. A. Imran, A. Alomainy, and Q. H. Abbasi, "Machine learning driven approach towards the quality assessment of fresh fruits using non-invasive sensing," *IEEE Sensors Journal*, vol. 20, no. 4, pp. 2075–2083, 2019.

[15] S. Tan, L. Zhang, and J. Yang, "Sensing fruit ripeness using wireless signals," in *2018 27th international conference on computer communication and networks (ICCCN)*. IEEE, 2018, pp. 1–9.

[16] Y. Liu, L. Jiang, L. Kong, Q. Xiang, X. Liu, and G. Chen, "Wi-fruit: See through fruits with smart devices," *Proceedings of the ACM on Interactive, Mobile, Wearable and Ubiquitous Technologies*, vol. 5, no. 4, pp. 1–29, 2021.

[17] C. A. Bennett, *Principles of physical optics*. John Wiley & Sons, 2022.

[18] A. Niaz, S. Khan, F. Niaz, M. U. Shoukat, I. Niaz, and J. Yanbing, "Smart city iot application for road infrastructure safety and monitoring by using digital twin," in *2022 International Conference on IT and Industrial Technologies (ICIT)*. IEEE, 2022, pp. 1–6.

[19] J. Weiß and A. Santra, "One-shot learning for robust material classification using millimeter-wave radar system," *IEEE sensors letters*, vol. 2, no. 4, pp. 1–4, 2018.

[20] S. O. Nelson, "Electrical properties of agricultural products-a critical review," *Transactions of the ASAE*, vol. 16, no. 2, pp. 384–0400, 1973.

[21] A. Niaz, M. U. Shoukat, Y. Jia, S. Khan, F. Niaz, and M. U. Raza, "Autonomous driving test method based on digital twin: A survey," in *2021 International Conference on Computing, Electronic and Electrical Engineering (ICE Cube)*. IEEE, 2021, pp. 1–7.

[22] D. Henry, H. Aubert, and T. Véronèse, "Proximal radar sensors for precision viticulture," *IEEE Transactions on Geoscience and Remote Sensing*, vol. 57, no. 7, pp. 4624–4635, 2019.

[23] F. Zidane, J. Lanteri, L. Brochier, N. Joachimowicz, H. Roussel, and C. Migliaccio, "Damaged apple sorting with mmwave imaging and nonlinear support vector machine," *IEEE Transactions on Antennas and Propagation*, vol. 68, no. 12, pp. 8062–8071, 2020.

[24] T. Tantisopharak, H. Moon, P. Youryon, K. Bunya-Athichart, M. Krairiksh, and T. K. Sarkar, "Nondestructive determination of the maturity of the durian fruit in the frequency domain using the change in the natural frequency," *IEEE Transactions on Antennas and Propagation*, vol. 64, no. 5, pp. 1779–1787, 2016.

[25] M. F. Adak and N. Yumusak, "Classification of e-nose aroma data of four fruit types by abc-based neural network," *Sensors*, vol. 16, no. 3, p. 304, 2016.

[26] D. El Khaled, N. Novas, J. A. Gazquez, R. M. Garcia, and F. Manzano-Agugliaro, "Fruit and vegetable quality assessment via dielectric sensing," *Sensors*, vol. 15, no. 7, pp. 15 363–15 397, 2015.

[27] J. Huang, B. Liu, C. Miao, X. Zhang, J. Liu, L. Su, Z. Liu, and Y. Gu, "Phyfinatt: An undetectable attack framework against phy layer fingerprint-based wifi authentication," *IEEE Transactions on Mobile Computing*, 2023.

[28] J. Huang, B. Liu, C. Miao, Y. Lu, Q. Zheng, Y. Wu, J. Liu, L. Su, and C. W. Chen, "Phaseanti: An anti-interference wifi-based activity recognition system using interference-independent phase component," *IEEE Transactions on Mobile Computing*, vol. 22, no. 5, pp. 2938–2954, 2021.

[29] N. Muramatsu, N. Sakurai, N. Wada, R. Yamamoto, K. Tanaka, T. Asakura, Y. Ishikawa-Takano, and D. J. Nevins, "Remote sensing of fruit textural changes with a laser doppler vibrometer," *Journal of the American Society for Horticultural Science*, vol. 125, no. 1, pp. 120–127, 2000.

[30] M. Zhou, Y. Zhou, S. Su, Q. Wang, Q. Li, S. Hu, C. Yu, and Z. Li, "Fingerpattern: Securing pattern lock via fingerprint-dependent friction sound," *IEEE Transactions on Mobile Computing*, 2023.

[31] Y. Cao, F. Li, H. Chen, X. Liu, S. Zhai, S. Yang, and Y. Wang, "Live speech recognition via earphone motion sensors," *IEEE Transactions on Mobile Computing*, 2023.

[32] H. Li, C. Xu, A. S. Rathore, Z. Li, H. Zhang, C. Song, K. Wang, L. Su, F. Lin, K. Ren *et al.*, "Vocalprint: A mmwave-based unmediated vocal sensing system for secure authentication," *IEEE Transactions on Mobile Computing*, vol. 22, no. 1, pp. 589–606, 2021.

[33] Y. Wang, Z. Wang, J. A. Zhang, H. Zhang, and M. Xu, "Vital sign monitoring in dynamic environment via mmwave radar and camera fusion," *IEEE Transactions on Mobile Computing*, vol. 23, no. 5, pp. 4163–4180,

2023.

[34] Y. Liang, P. Shi, Z. Zheng, L. Pu, and A. Zhou, "mm-taster: a mobile system for fine-grained and robust alcohol sensing," *IEEE Transactions on Mobile Computing*, 2023.

[35] F. Shang, P. Yang, Y. Yan, and X.-Y. Li, "Contactless and fine-grained liquid identification utilizing sub-6ghz signals," *IEEE Transactions on Mobile Computing*, 2023.

[36] F. Niaz, J. Zhang, M. Khalid, K. N. Qureshi, Y. Zheng, M. Younas, and N. Imran, "Ai enabled: a novel iot-based fake currency detection using millimeter wave (mmwave) sensor," *Computing*, vol. 106, no. 8, pp. 2851–2873, 2024.

[37] F. Niaz, J. Zhang, Y. Zheng, M. Khalid, and A. Niaz, "mm-cur: A novel ubiquitous, contact-free, and location-aware counterfeit currency detection in bundles using millimeter-wave sensor," *ACM Transactions on Sensor Networks*, 2024.

[38] N. Jabeen, R. Hao, A. Niaz, M. U. Shoukat, F. Niaz, and M. A. Khan, "Autonomous vehicle health monitoring based on cloud-fog computing," in *2022 International Conference on Emerging Trends in Electrical, Control, and Telecommunication Engineering (ETECTE)*. IEEE, 2022, pp. 1–6.

[39] A. K. Datta, G. Sumnu, and G. Raghavan, "Dielectric properties of foods," in *Engineering properties of foods*. CRC Press, 2014, pp. 523–588.

[40] M. Schwartz, *Principles of electrodynamics*. Courier Corporation, 2012.

[41] F. Niaz, M. Khalid, Z. Ullah, N. Aslam, M. Raza, and M. Priyan, "A bonded channel in cognitive wireless body area network based on ieee 802.15. 6 and internet of things," *Computer Communications*, vol. 150, pp. 131–143, 2020.

[42] A. Niaz, M. S. Kader, S. Khan, Y. Jia, M. U. Shoukat, S. A. Nawaz, F. Niaz, and I. Niaz, "Environment friendly hybrid solar-hydro power distribution scheduling on demand side," *Polish Journal of Environmental Studies*, vol. 32, no. 1, pp. 215–224, 2022.

[43] Y. Yan, S. Zhang, Y. Jin, F. Cheng, Z. Qian, and S. Lu, "Spatial and temporal detection with attention for real-time video analytics at edges," *IEEE Transactions on Mobile Computing*, 2024.

[44] R. Fu, H. Liang, S. Wang, C. Jia, G. Sun, T. Gao, D. Chen, and Y. Wang, "Transformer-bls: An efficient learning algorithm based on multi-head attention mechanism and incremental learning algorithms," *Expert Systems with Applications*, vol. 238, p. 121734, 2024.

[45] W. Ruan, Q. Z. Sheng, P. Xu, L. Yang, T. Gu, and L. Shangguan, "Making sense of doppler effect for multi-modal hand motion detection," *IEEE Transactions on Mobile Computing*, vol. 17, no. 9, pp. 2087–2100, 2017.

[46] T. Instruments, "Iwr1443," https://www.ti.com/lit/gpn/iwr1443, accessed: 2024-11-06.

[47] M. Tan and Q. Le, "Efficientnet: Rethinking model scaling for convolutional neural networks," in *International conference on machine learning*. PMLR, 2019, pp. 6105–6114.

[48] L. Wen, X. Li, and L. Gao, "A transfer convolutional neural network for fault diagnosis based on resnet-50," *Neural Computing and Applications*, vol. 32, no. 10, pp. 6111–6124, 2020.

Fahim Niaz is currently a Ph.D. scholar at Wuhan University, China, and received his M.S. in Computer Science from Bahria University, Islamabad, Pakistan, in 2018. From 2017 to 2022, he served as a Lecturer at Higher Education Khyber-Pakhtunkhwa. His research interests include the Internet of Things (IoT), Wireless Sensor Networks, and Millimeter-Wave Radars. Fahim also works as an AI expert at Wuhan University's Institute of Artificial Intelligence, specializing in transfer learning and advanced deep learning models.

Jian Zhang received the B.S., M.S., and Ph.D. degrees in computer architecture from Wuhan University, Wuhan, China, in 1998, 2001, and 2006, respectively. He is currently a professor in the School of Computer Science at Wuhan University. His research interests include Cloud Computing, the Internet of Things (IoT), and Big Data.

Muhammad Khalid is currently a Lecturer (Assistant Professor) in Computer Science at the School of Computer Science, University of Hull. Previously, he was a Post-Doctoral Research Fellow at the University of Lincoln, where he focused on ensuring robot autonomy with respect to safety considerations. He completed his Ph.D. in 2020 at Northumbria University, specializing in autonomous parking in intelligent smart cities.

Muhammad Younas received his Master's degree in Software Engineering from Northeastern University, China, in 2022. He is currently pursuing a Ph.D. at the School of Computer Science, Wuhan University, China. His research interests include the Internet of Things (IoT), Wireless Sensor Networks, Millimeter-Wave Radars, Artificial Intelligence, Machine Learning, and Blockchain.

Ashfaq Niaz received his Ph.D. degree in Electrical Engineering from Taiyuan University of Technology, Shanxi, China. His research interests include Control Systems Engineering, Electrical Engineering, Computer Engineering, Smart Grids, Autonomous Vehicles, Renewable Energy (Solar and Wind), Digital Twins, 5G Technology, Artificial Intelligence, Deep Learning, and Machine Learning.